

10<sup>th</sup> ANKARA INTERNATIONAL AEROSPACE CONFERENCE  
18-20 September 2019 - METU, Ankara TURKEY

**AIAC-2019-156**

## **COMPOSITE ROCKET FIN OPTIMIZATION BASED ON FLUTTER ANALYSIS**

Sinan GÖZÜM<sup>1</sup> and Arif Emre ÖRÜN<sup>2</sup>  
GAZI University  
Ankara, Turkey

Elmas SALAMCI<sup>3</sup>  
GAZI University  
Ankara, Turkey

### **ABSTRACT**

*In this study, rocket fin design is presented in terms of flutter analysis, which is very critical for thin-walled and one-sided fixed aircraft parts like wing, tail and fin. The study has been carried out using composite material which has been increasing rapidly in the aviation field in the last 30 years. Analysis for using fin design were verified by using NACA test results, theoretical calculations and another FE program. For carbon fiber, epoxy glass and graphite epoxy materials [Rajadurai et al, 2017], approximately 100 analyzes were carried out for different orientation angles and number of layers. In this way, it is aimed to provide the optimum fin design according to the index of resistance to flutter/structure weight. In terms of strength against to flutter, the strongest material is carbon, so when we include the weight/density factor, it can be said that graphite epoxy is as efficient as carbon fiber.*

### **INTRODUCTION**

Flutter is a dangerous phenomenon encountered in flexible structures subjected to aerodynamic forces. This includes wing of aircraft, buildings, and bridges. Flutter occurs as a result of interactions between aerodynamics, stiffness/structural design and inertial forces on a structure. In an aircraft, as the speed of the wind increases, there may be a point at which the structural damping is insufficient to damp out the motions which are increasing due to aerodynamic energy being added to the structure. This vibration can cause structural failure and therefore considering flutter characteristics is an essential part of designing an aircraft [Velmurugan, 2013].

#### **Composite in aircraft**

The first generation of conventional powered aircraft was constructed of wood and canvas. Then aluminum and steel alloy was the used in aircraft construction. The increased loadings and complex structural forms of present day aircrafts cause high stress concentrations for which the conventional material is not well adapted. Nowadays, the composite materials have replaced the traditional metals [Mathai, 2014].

During the design of air vehicles; since the strength of the structure as well as the lightness is a very important factor, composite parts are used as much as possible. Especially in the 1980s, the trend of composite usage, which started with using fighter aircraft, increased rapidly. On Airbus A350 and Boeign B787 type passenger aircraft, the composite ratio has reached 50% of the total weight of the aircraft.

---

<sup>1</sup> MSc. Student in a Mechanical Engineering, gozumsinan@gmail.com

<sup>2</sup> PhD. Student in a Mechanical Engineering, arifemreorun@gmail.com

<sup>3</sup> Assoc. Dr. in a Mechanical Engineering, esalamci@gazi.edu.tr

## METHOD

When the thesis and articles are investigated, flutter analysis for metal structures or composite material design in aircraft structures related to structural strength are observed. However, study on the choice of composite materials and design related to the flutter criterion in wing or fin structures is not encountered. The aim of this paper is to determine the flutter-efficient composite fin design following the steps:

- I. Finite element modeling (FEM) for flutter analysis carried out Siemens FEMAP program will be verified using the test results and hand calculations for metal fins in literature studies.
- II. Composite fins designed by using different composite materials, lay-up orientations and number of layers will be evaluated and the result will be compared for each designs.

During the study, the test results in RM SL58H08 “Experimental investigation of flutter and divergence characteristics of the rocket-motor fin of the ASROC missile” [NACA-1, 1958] published by NACA and the theoretical equations in NACA Technical Note 4197 “Flutter Experience as a Guide to the Preliminary Design of Lifting Surfaces on Missiles” [NACA-2, 1958] are taken as reference. Material properties and geometric parameters of ASROC fin are presented in Figure 1 and Table 1.

Half-scale: all dimensions in inches

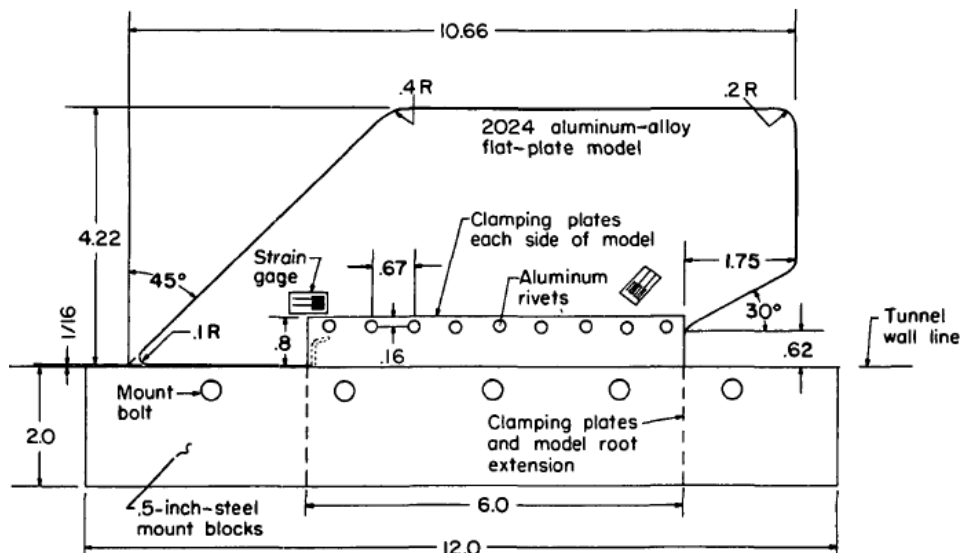


Figure 1: ASROC Fin Geometry

Table 1: Aluminum 2024 Material properties and geometric parameters of ASROC

$E$	10000000	[psi]	Young's Modulus
$\nu_e$	0.33	-	Poisson's Ratio
$G$	3759398	[psi]	Shear Modulus
$c_r$	8.91	[in]	Root Chord
$c_t$	6.44	[in]	Tip Chord
$c_{mean}$	7.68	[in]	Mean Chord
$b$	3.42	[in]	Semi-Span
$t$	0.05	[in]	Thickness
$S$	26.25	[in <sup>2</sup> ]	Fin Area
$AR$	0.45	[-]	Aspect Ratio
$\lambda$	0.72	[-]	Tip to Root Ratio

Flutter tests were carried out by NACA at different altitudes and test results are presented in Table 2. Air density, temperature, sound velocity and pressure parameters varying according to altitude are modeled in finite element analysis as a boundary condition. Test-38 result from Table 2 is selected to validate FE modelling.

Table 2: ASROC Test Result for different conditions

Test	Model	t, in.	Frequency, cps					M	T, °R	ρ, slugs/cu ft	a, fps	q, lb/sq ft	Legend (a)
			f <sub>1</sub>	f <sub>2</sub>	f <sub>3</sub>	f <sub>4</sub>	f <sub>F</sub>						
33	BF-10A	0.050	114	170	---	310	155	1.30	542	0.00183	986	1,507	F
19	BF-7C	.050	113	164	250	300	145	.60	559	.00246	1,123	887	F
5	BF-2	.072	147	234	400	455	---	1.30	544	.00424	988	3,500	Q
6	BF-3	.063	137	215	350	410	---	1.30	532	.00378	977	3,060	Q
18	BF-2	.072	150	233	430	460	---	.60	566	.00552	1,130	1,264	Q
21	BF-2	.072	148	234	406	460	---	.96	536	.00574	1,044	2,865	Q
34	BF-3	.063	128	213	352	420	---	1.30	545	.00378	989	3,125	Q
37	BF-13	.050	130	213	---	392	---	1.30	555	.00356	999	3,000	Q
38	BF-13A	.050	133	214	---	380	225	1.30	556	.00338	999	2,850	F
39	BF-14	.050	128	184	---	336	162	1.30	552	.00220	995	1,846	F
40	BF-15	.050	128	197	---	363	172	1.30	548	.00288	992	2,400	F

As the theoretical calculation, equation-18 in NACA Technical Note 4197 was used.

$$\left(\frac{V_f}{a}\right)^2 = \frac{G_E}{\frac{39.3A^3}{\left(\frac{t}{c}\right)^3 (A+2)} \left(\frac{\lambda+1}{2}\right) \left(\frac{p}{p_0}\right)}$$

Where,

$V_f$  : Flutter speed,

$a$  : Speed of sound,

$G_E$ : Shear modulus,

$A$  : Aspect ratio,

$t$  : Fin thickness,

$c$  : root chord,

$\lambda$  : tip to root ratio,

$p$  : Pressure,

The Siemens FEMAP program was used in the finite element analysis (FEA) and the process is defined in five steps as follows:

- Creation of Geometry: Fin geometry is formed in CATIA v5 shown in Figure 2 and imported to FEMAP as Step format.

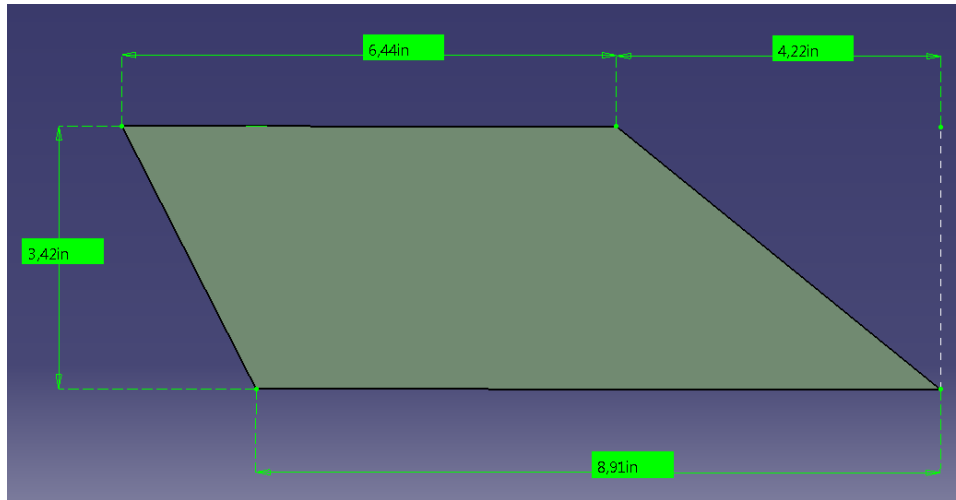


Figure 2: Fin Geometry model in CATIA v5

- b. Assigning Material and Property (property): The analyzes were carried out in 2-D shell model. The values in Table 1 were used as thickness and material.
- c. Determination of Boundary Conditions: Fin is rigidly connected to the rocket and is modeled as a fixed from its root chord. In the 38th test case result, it is seen that the sound speed is 999 fps and the altitude to reach this speed is calculated as 29000 ft. The ratio of density of the air calculated at this altitude and sea level was entered as the ambient condition.
- d. Assigning Mesh: Two types of solution mesh are used in aeroelastic/flutter analysis shown in Figure 3. For deciding mesh size, mesh convergence process was conducted and shown in Figure 4 and Table 3.

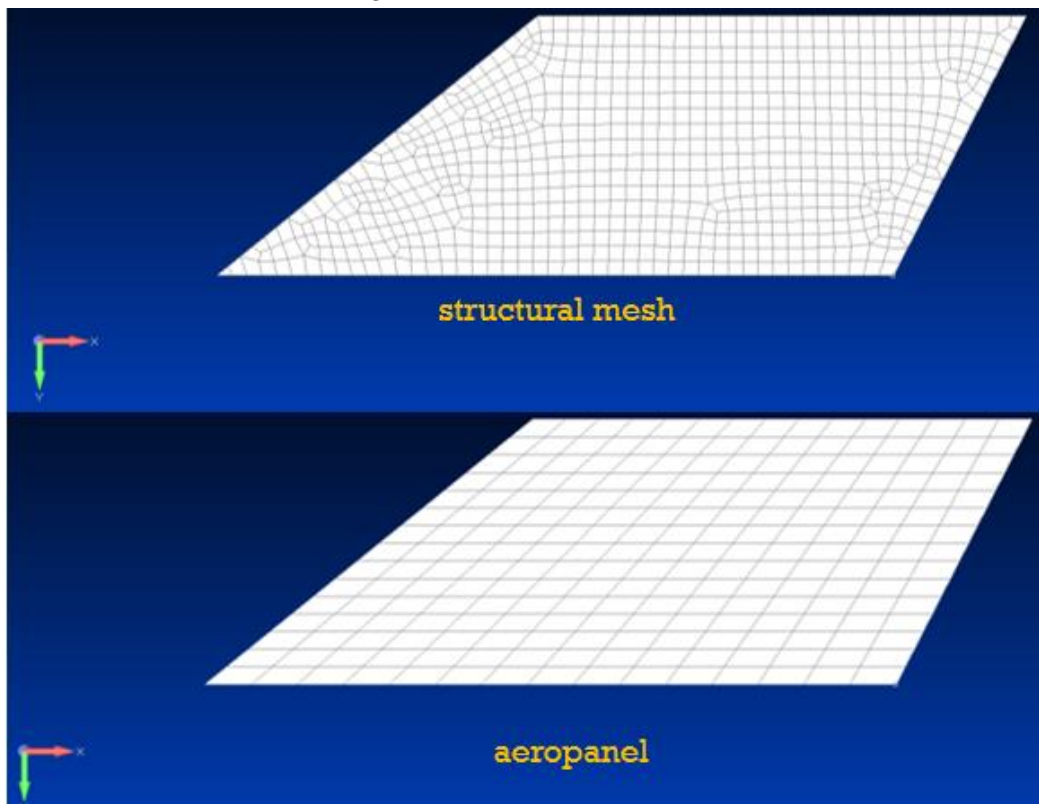


Figure 3: Structural and Aeropanel Mesh in FEMAP

Table 3: Mesh Convergence w.r.t Number of Aero and Structural Element

# of AeroPanel Element	Flutter Speed [ft/s] w.r.t. Structural Mesh Size [inch]		
	0.1	0.2	0.3
100	1255.1	1255.8	1251.9
225	1270.3	1269.1	1265.1
400	1276.7	1275.2	1270.9
625	1280.4	1278.5	1274.6
1225	1284.3	1282.6	1279.2
2500	1287.0	1286.0	1282.6

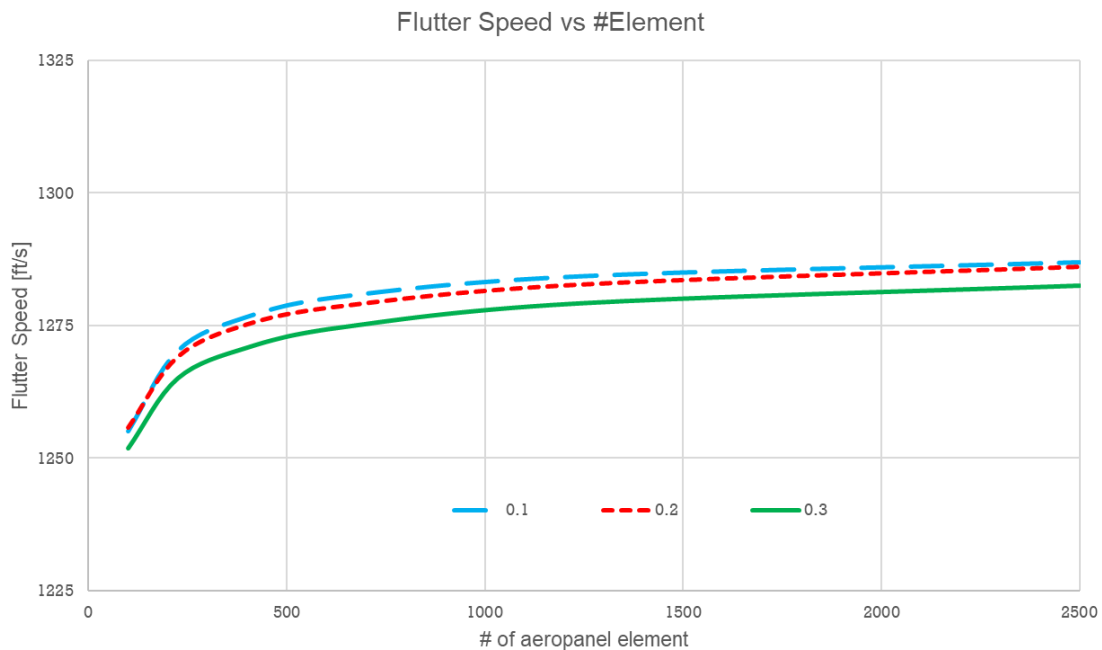


Figure 4: Mesh Convergence Graph

While structural mesh represents the fin strength, aeropanel mesh is used to define aerodynamics loads. From Figure 4 and Table 3, the element size for structural is taken as 0.2 inches and the size of the aeropanel element is selected as 0.4 inches. The loads from aerodynamic effects were transferred from the aeropanel to the structural mesh using «spline» method.

- e. Reading the results from \*.op2 and \*.f06 outputs: Flutter occurs when the damping rate (read from the f06 output files) passes from negative to positive. Damping ratio curves is shown in Figure 5. While the first mode (red line) does not pass to the positive section, it is seen that the 2nd Mode (blue line) has cut the axis in the order of 1270 ft/s (it is also display in Figure 6).

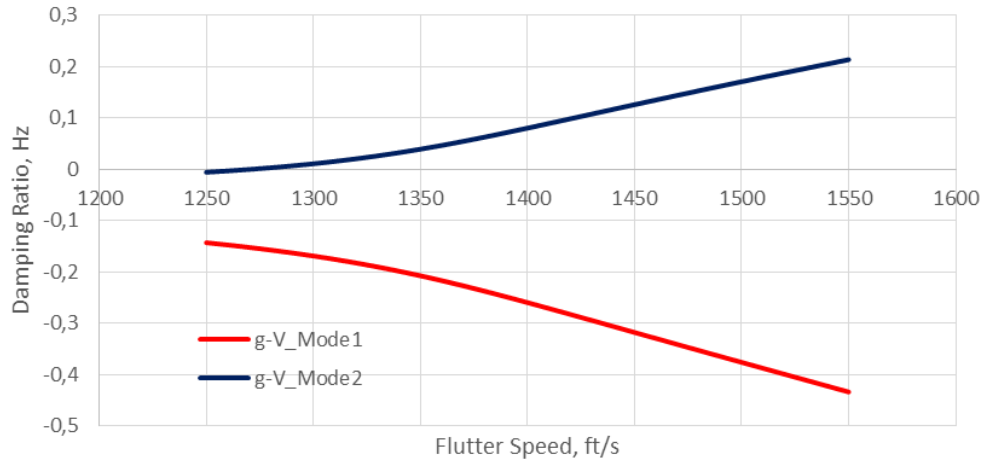


Figure 5: Flutter Speed vs Damping Ratio

FLUTTER SUMMARY					
POINT =	2	CONFIGURATION = AEROSG2D	XY-SYMMETRY = ASYMMETRIC	KZ-SYMMETRY = ASYMMETRIC	METHOD = PK
		MACH NUMBER = 0.8000	DENSITY RATIO = 3.8885E-01		
KFREQ	1./KFREQ	VELOCITY	DAMPING	FREQUENCY	COMPLEX
0.1170	8.5472870E+00	1.2000000E+03	-1.4700398E-02	9.7809706E+00	-4.5171130E-01
0.1169	8.5567875E+00	1.2010000E+03	-1.4558055E-02	9.7782526E+00	-4.4721305E-01
0.1167	8.5663013E+00	1.2020000E+03	-1.4414149E-02	9.7755260E+00	-4.4266894E-01
0.1166	8.5758247E+00	1.2030000E+03	-1.4268657E-02	9.7727938E+00	-4.3807825E-01
0.1165	8.5853596E+00	1.2040000E+03	-1.4121586E-02	9.7700539E+00	-4.3344131E-01
0.1163	8.5949068E+00	1.2050000E+03	-1.3972896E-02	9.7673073E+00	-4.2875695E-01
0.1162	8.6044655E+00	1.2060000E+03	-1.3822562E-02	9.7645531E+00	-4.2402434E-01
0.1161	8.6140366E+00	1.2070000E+03	-1.3670592E-02	9.7617922E+00	-4.1924390E-01
0.1160	8.6236181E+00	1.2080000E+03	-1.3516953E-02	9.7590246E+00	-4.1441464E-01
0.1158	8.6332121E+00	1.2090000E+03	-1.3361595E-02	9.7562485E+00	-4.0953502E-01
0.1157	8.6428175E+00	1.2100000E+03	-1.3204571E-02	9.7534666E+00	-4.0460679E-01
0.1156	8.6524363E+00	1.2110000E+03	-1.3045784E-02	9.7506762E+00	-3.9962700E-01
0.1154	8.6620655E+00	1.2120000E+03	-1.2885282E-02	9.7478790E+00	-3.9459714E-01
-----					
0.1121	8.9167538E+00	1.2380000E+03	-8.0260411E-03	9.6725912E+00	-2.4389006E-01
0.1120	8.9267216E+00	1.2390000E+03	-7.8097177E-03	9.6695957E+00	-2.3724307E-01
0.1119	8.9367008E+00	1.2400000E+03	-7.5909784E-03	9.6665936E+00	-2.3052663E-01
0.1118	8.9466934E+00	1.2410000E+03	-7.3697600E-03	9.6635838E+00	-2.2373886E-01
0.1116	8.9567003E+00	1.2420000E+03	-7.1460605E-03	9.6605654E+00	-2.1687980E-01
0.1115	8.9667196E+00	1.2430000E+03	-6.9198306E-03	9.6575403E+00	-2.0994806E-01
0.1114	8.9767523E+00	1.2440000E+03	-6.6910745E-03	9.6545076E+00	-2.0294385E-01
0.1113	8.9867964E+00	1.2450000E+03	-6.4597386E-03	9.6514683E+00	-1.9586563E-01
0.1111	8.9968557E+00	1.2460000E+03	-6.2257815E-03	9.6484213E+00	-1.8871222E-01
0.1092	9.1595993E+00	1.2620000E+03	-2.1006658E-03	9.5986881E+00	-6.3345931E-02
0.1091	9.1698828E+00	1.2630000E+03	-1.8172185E-03	9.5955200E+00	-5.4780442E-02
0.1089	9.1801815E+00	1.2640000E+03	-1.5305307E-03	9.5923452E+00	-4.6122916E-02
-----					
0.1082	9.2422457E+00	1.2700000E+03	2.5983487E-04	9.5731573E+00	7.8145238E-03
0.1081	9.2526360E+00	1.2710000E+03	5.7028123E-04	9.5699358E+00	1.7145416E-02
0.1080	9.2630386E+00	1.2720000E+03	8.8427891E-04	9.5667095E+00	2.6576743E-02
0.1078	9.2734556E+00	1.2730000E+03	1.2018975E-03	9.5634766E+00	3.6110468E-02
0.1077	9.2838840E+00	1.2740000E+03	1.5231272E-03	9.5602369E+00	4.5746170E-02

Figure 6: f06 output files

In Table 4, the results of flutter speed obtained from FEMAP program and theoretical calculus, and the difference of these results with NACA test data are presented. The differences are below 5% indicates that the finite element analysis and the theoretical approach are acceptable. In the mesh convergence study, it is seen that it is possible to reduce the difference to less than 1% by improving the aeropanel size used in FEA analyzes, but in this case, the duration of solution is become longer.

Table 4: Comparison ASROC Test Result, Theoretical Calculation and FEMAP FEA Result

Method	$V_f$ Flutter Speed [ft/sec]	Difference between test result
Test	1298.7	%0.00
Theoretical	1318.6	+%1.53
FEA	1270.0	-%2.21

An example FEMAP fin view which is exposed to flutter is presented in Figure 7.

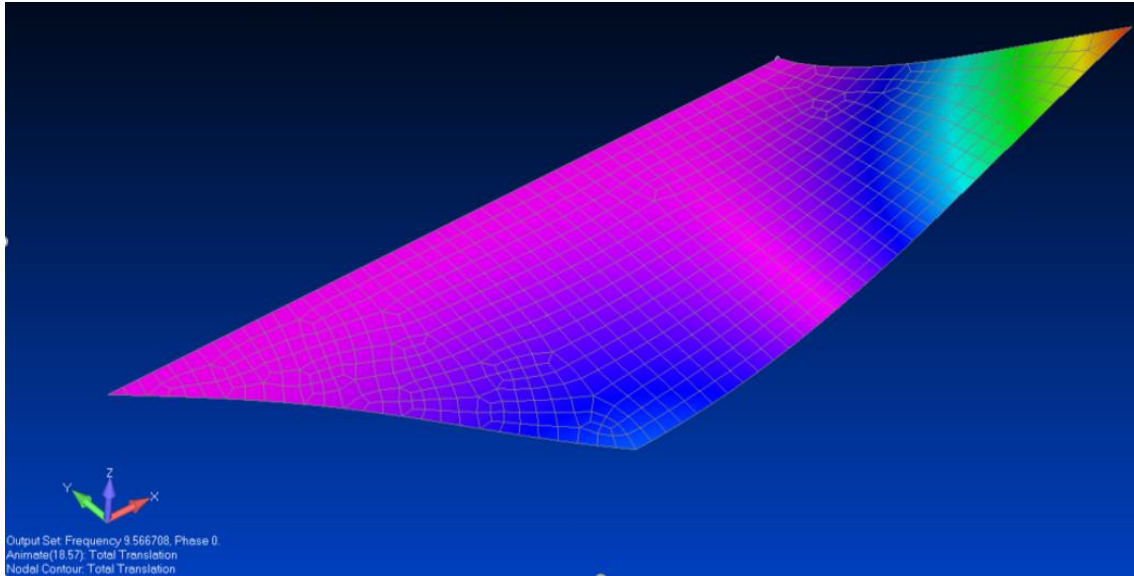


Figure 7: Flutter view in FEMAP

### Composite Fin Optimization

Firstly, reference [Velmurugan and Vadivel, 2013; Mathai, 2014 and Jones, 1999] were used to select the composite materials to be used in the fin design, and properties of these materials are shown in Table 5. As is known, composite materials have orthotropic properties and their properties in all direction are entered into the finite element program. Carbon-Fiber Reinforced Polymer (CFRP), E-Glass and Graphite Epoxy materials were selected to compare each other with respect to flutter phenomena. These materials are used in many parts of passenger and combat aircraft, frequently.

Table 5: Mechanical Properties of selected Composite Materials

	E-Glass [9]	CFRP (M55j/914 prepreg) [8]	Graphite Epoxy [9]	Unit	
$\rho$	0.072	0.064	0.057	[lb/in <sup>3</sup> ]	Density
$E_1$	7800000	39160189	30000000	[psi]	Young's Modulus (longitudinal)
$E_2$	2600000	802784	750000	[psi]	Young's Modulus (transverse)
$G_{12}$	1300000	561296	375000	[psi]	Shear Modulus (inplane)
$\nu_e$	0.25	0.365	0.25	-	Poisson's Ratio
$\sigma_{ty1}$	150000	261068	150000	[psi]	Tensile strength (longitudinal)
$\sigma_{ty2}$	4000	3191	6000	[psi]	Tensile strength (transverse)
$\sigma_{cy}$	150000	87023	100000	[psi]	Compressive strength
$\tau_{sy}$	6000	13343	10000	[psi]	Shear Strength

In the first part, hand calculations and test results by using metal material (Aluminum) were verified in Femap program. At this stage, firstly, orthotropic aluminum material with 8-layer and single-orientation was modeled in Femap as composite. Then, the obtained results was compared with result of the same thickness aluminum which was isotopically modeled. In the studies carried out in different element sizes, the results were occurred same for orthotropic and isotropic aluminum. In this way, the composite module of Femap was verified

(Flutter test studies by using the composite material which are similar to given in references 2 and 3 was not found).

Since there are no rib and spar structures in the fin, all the loads coming to the system are carried by the fin. Therefore, all orientation possibilities were evaluated during layering.

The thickness of lamina is 0.05 inch as in ASROC Fin. Number of layers was selected as 8, 10 and 12 were taken in symmetrically. The thickness of each layer (ply) were 0.00625, 0.0050 and 0.00417 inches, respectively.

27 different orientations were determined for laminate with 8 plies and analyzes were performed using E-Glass material. As a result of analyzes, seven different sequences will be determined for each laminates with 10 and 12 plies, depending on the load path.  $0^\circ$  direction is taken as the Y axis of the fin model given in Figure 8.

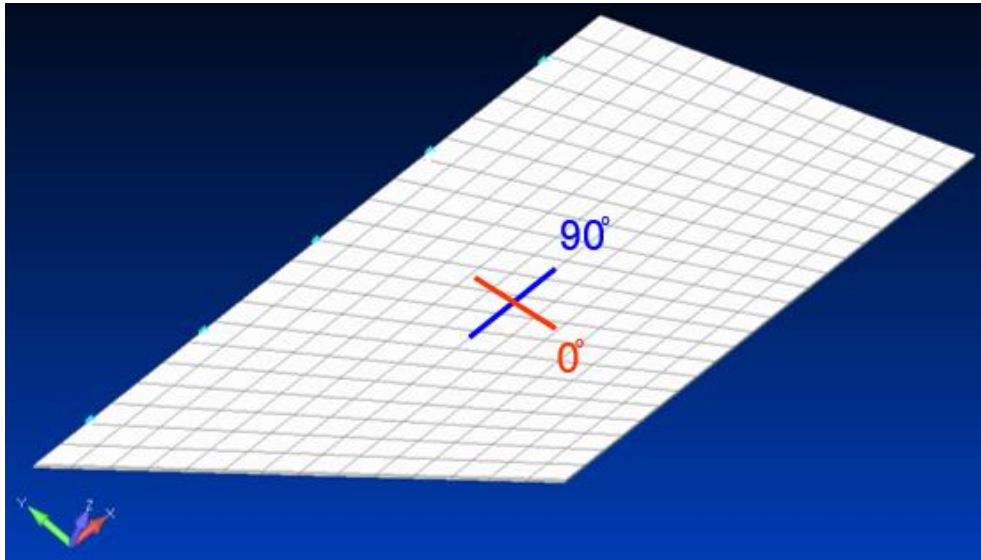
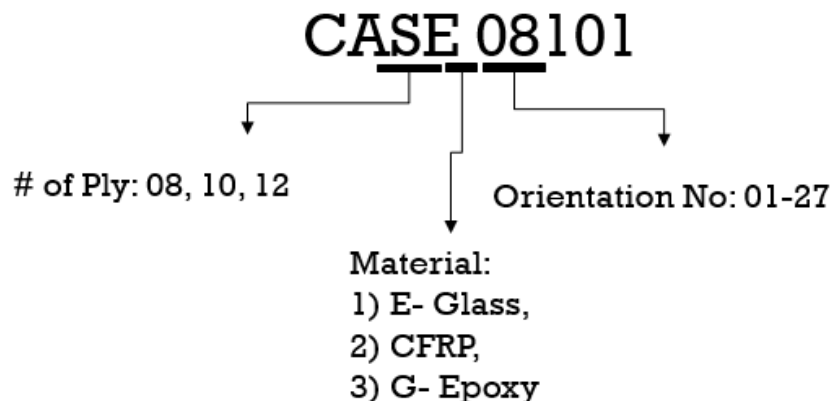


Figure 8: Ply Orientation

For the E-Glass material, 41 different analyzes were carried out with analyzes for laminates with 10 and 12 plies. With these analyzes, the effects of layer number and orientation were examined. Since the number of configurations to be analyzed is numerous, the following notation has been created to facilitate the examination of the results.



**RESULTS AND DISCUSSION**

Flutter speeds were obtained in analyzes, carried out with 27 different orientations for E-Glass laminate with 8 plies shown in Figure 9.



Figure 9: Flutter Results for 8-plyes E-Glass Fin at 27 different orientations

At the top ply of fins with 90° and 45° orientations have the highest flutter speed shown in Figure 9. As a result of these analyzes, number of orientation for 10 and 12 layers are reduced to seven and the results are presented in Figure 10.

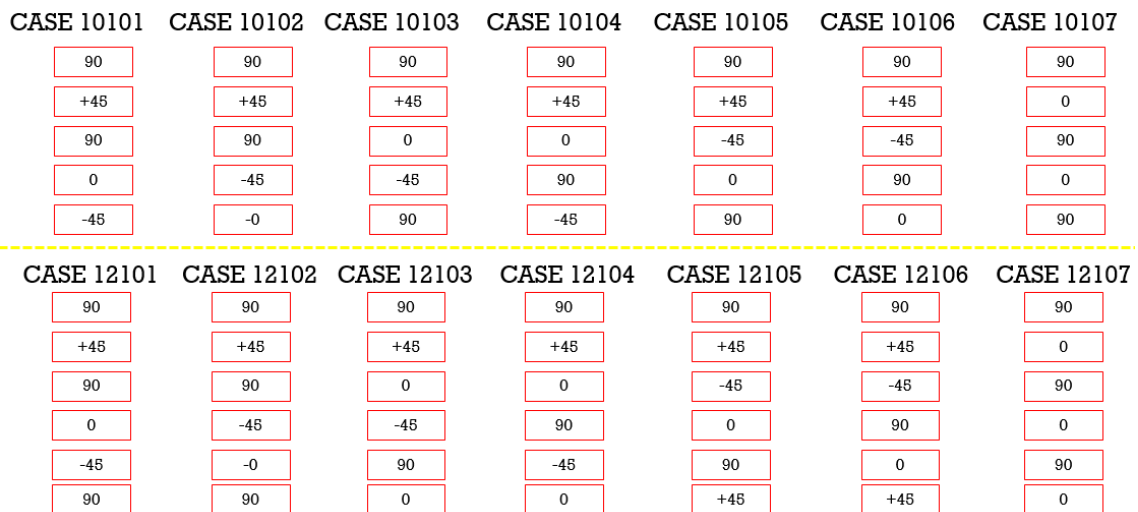


Figure 10: Flutter Results for 10 and 12-plyes E-Glass Fin at 7 different orientations

The best 7 results of the flutter speed, carried out for laminates with 8, 10 and 12 plies for the E-glass materials, are compared in Table 6,.

Table 6: Comparison for the Highest Flutter Speeds of 8, 10 and 12 plies E-Glass Fin

CASE #	Flutter Speed [ft/s]	CASE #	Flutter Speed [ft/s]	CASE #	Flutter Speed [ft/s]
CASE 08105	1769	CASE 10101	1774	CASE 12101	1757
CASE 08106	1743	CASE 10102	1787	CASE 12102	1772
CASE 08107	1690	CASE 10103	1710	CASE 12103	1693
CASE 08115	1797	CASE 10104	1723	CASE 12104	1709
CASE 08116	1747	CASE 10105	1735	CASE 12105	1715
CASE 08117	1694	CASE 10106	1761	CASE 12106	1746
CASE 08126	1710	CASE 10107	1689	CASE 12107	1679

It is seen that the results obtained for different layer numbers and orientations are very close to each other. It can be said that the number of layers has no significant effect on flutter velocity. Therefore, in the material comparison section, analyzes will be performed for only 8-layered sequences.

For CFRP (M55j/914 prepreg) and Graphite Epoxy materials, flutter analyzes were performed in different orientations. In analyzes carried out with E-Glass material, it was observed that the highest flutter speeds were achieved with 90° orientation in the upper layer. However, since the transverse modulus values for these materials are lower than E-Glass, the maximum flutter speed was observed when the 45° layer was at the top. Depending on these results, new orientations were made considering the possibilities of 45° layer for the upper layer and shown in Figure 11.

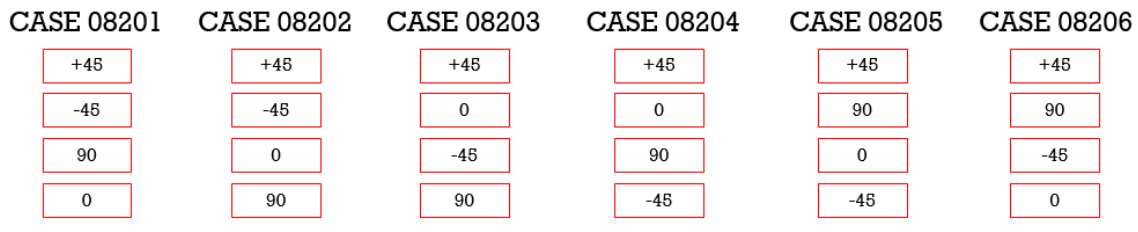


Figure 11: Ply orientations for CFRP and Graphite Epoxy

For E-Glass, CFRP (M55j/914 prepreg) and Graphite Epoxy materials, the six cases with the highest flutter speed are presented in Table 7.

Table 7: Comparison for E-Glass, CFRP and G-Epoxy w.r.t. Flutter Speed

CASE # for E-Glass	Flutter Speed [ft/s]	CASE # for CFRP	Flutter Speed [ft/s]	CASE # Graphite Epoxy	Flutter Speed [ft/s]
CASE 08105	1769	CASE 08201	2029	CASE 08301	1783
CASE 08106	1743	CASE 08202	2046	CASE 08302	1799
CASE 08115	1797	CASE 08203	1768	CASE 08303	1556
CASE 08116	1747	CASE 08204	1608	CASE 08304	1415
CASE 08117	1694	CASE 08205	1512	CASE 08305	1331
CASE 08126	1710	CASE 08206	1668	CASE 08306	1468

## CONCLUSIONS

- In the analysis carried out with Al2024 material, the flutter speed was approximately 1300 ft/s. This value is percent of lower than result for E-Glass and G-Epoxy; it is also percent of 58 lower than the CFRP result.
- Maximum flutter speed of CFRP (M55j/914 prepreg) is about 12% higher than the flutter speed of other two composite materials.
- When the result of the E-Glass and Graphite Epoxy were compared, there was no significant difference between them in terms of flutter. Since the density of Graphite Epoxy is less than E-Glass, it will be possible to make a lighter design with Graphite. Therefore, Graphite Epoxy can be preferred instead of E-Glass.
- The density of CFRP (M55j/914 prepreg) is about 10% higher than Graphite Epoxy. Considering about flutter speed - lightweight design, both of composite materials can be preferable.

As a result of this study, flutter or lightness can be selected whichever is more critical, or different preference parameters, such as price of composite material and ease of supply, can be considered.

## References

1. Jones, R. (1999) *“Mechanics of Composite Materials”* Taylor & Francis, USA
2. Mathai, A. and Kurian, A. (2014) *Ply Orientation of Carbon Fiber Reinforced Aircraft Wing - A Parametric Study*. Journal of Engineering Research and Applications.
3. NACA, (1958) *Experimental investigation of flutter and divergence characteristics of the rocket-motor fin of the ASROC missile*, National Advisory Committee for Aeronautics, Washington.
4. NACA, (1958) *Flutter Experience as a Guide to the Preliminary Design of Lifting Surfaces on Missiles*, National Advisory Committee for Aeronautics, Washington.
5. Rajadurai, M. et al (2017) *Optimization of Ply Orientation of Different Composite Materials for Aircraft Wing*, International Journal of Advanced Engineering Research and Science (IJAERS).
6. Velmurugan, G. and Vadivel, D. (2013) *Study of Flutter Analysis on Composite Plate Structure*. International Journal of Scientific & Engineering Research.